

Semiclassical ordering in the large- N pyrochlore antiferromagnet

U. Hizi,^{1,*} Prashant Sharma,^{1,2} and C. L. Henley¹

¹Laboratory of Atomic and Solid State Physics, Cornell University, Ithaca, NY, 14853-2501

²Argonne National Laboratory, Materials Science Division, Argonne, IL, 60439

We study the semiclassical limit of the $Sp(N)$ generalization of the pyrochlore lattice Heisenberg antiferromagnet by expanding about the $N \rightarrow \infty$ saddlepoint in powers of a generalized inverse spin. To leading order, we write down an effective Hamiltonian as a series in loops on the lattice. Using this as a formula for calculating the energy of any classical ground state, we perform Monte Carlo simulations and find a unique collinear ground state. This state is not a ground state of linear spin-wave theory, and can therefore not be a physical ($N = 1$) semiclassical ground state.

PACS numbers: 75.10.Jm, 75.25.+z, 75.50.Ee

Geometrically frustrated antiferromagnets [1, 2] have attracted interest because their large classical ground state degeneracy can allow a rich variety of correlated states, including (at $T = 0$) quantum spin liquids or complex ordered states. The simplest examples are nearest-neighbor, exchange-coupled antiferromagnets in which spins form triangles or tetrahedra that share corners [3]: the kagomé, “checkerboard”, and SCGO ($\text{SrCr}_{9p}\text{Ga}_{12-9p}\text{O}_{19}$) lattices [1] in two dimensions, plus the garnet and pyrochlore lattices in three dimensions: the pyrochlore, in particular, consists of tetrahedra whose centers form a diamond lattice. The Hamiltonian is $H = \sum J_{ij} \mathbf{S}_i \cdot \mathbf{S}_j$, where $J_{ij} = 1$ for nearest neighbors $\langle ij \rangle$. In fact, additional terms – dipole interactions and anisotropies (as in $\text{Gd}_2\text{Ti}_2\text{O}_7$), magnetoelastic couplings (as in ZnV_2O_4 and ZnCr_2O_4) – decide the order in most real materials [1, 2]. Still, the case with pure Heisenberg exchange is worth understanding since (i) most simulations are done for this case; (ii) the more realistic systems emerge from it by the addition of perturbations; (iii) this has motivated experimentalists to search for model systems in which the aforementioned perturbations are small; (iv) quantum effects can be studied without being overshadowed by classical effects.

What is the ground state for large spin length S ? In unfrustrated antiferromagnets, it is just the classical ground state dressed with zero-point fluctuations of harmonic spin waves, and in frustrated cases the spin-wave zero-point energy *may* lift the degeneracy of classical ground states [4]. In the pyrochlore case, though, a large degeneracy remains [5]; its resolution by higher-order (anharmonic) terms in the semiclassical ($1/S$) expansion requires arduous approximations [6].

An established alternative to the spin-wave approach is to generalize the Heisenberg spins [with $SU(2) \cong Sp(1)$ symmetry] to $Sp(N)$ symmetry [7]: here N is the number of flavors of Schwinger bosons whose bilinear form represents a *generalized spin* [7], with length $\kappa = 2S$. The resulting mean-field theory (valid in the $N \rightarrow \infty$ limit) is popular as an analytic approach to the $S = 1/2$ limit, since the *small- κ* limit captures various disordered and exotic ground states [7, 8]. The large- N mean-field theory is also useful at *large- κ* for this paper’s problem, since it gives a simple analytical prescription for ground state selection: unlike the spin-wave expansion, here all degeneracies are (typically) broken at the lowest order

der [$\mathcal{O}(1/\kappa)$] quantum correction [7, 9].

However, on highly frustrated lattices this approach has the complication of a macroscopic (exponential) number of degenerate saddle-points not related by symmetry, so it is unknown a priori which of these should be expanded around; this was handled till now by limiting the investigation to ordering patterns of high symmetry and small magnetic cells, or by enumerating all saddle-points in a small finite system [9, 10].

In this letter, we develop an *effective Hamiltonian* [3] approach to this question. The pertinent saddle-points are labeled by arrangements of valence bond variables, and we obtain a simple formula for the large- N mean-field energy of *any* classical ground state, as a function of these variables. The effective Hamiltonian is constructed as an analytical real-space expansion of *loops* made of valence bonds. This allows us to systematically search for a collinear pyrochlore ground state, using Monte Carlo annealing, on quite large system sizes. However, we also find that the pyrochlore ground state does *not* agree with even the lowest-order term in the spin-wave expansion, and therefore cannot give the right answer for the physical ($N = 1$) ground state, in the large- S limit, demonstrating a limitation of the large- N approach for this case.

Large N mean field theory.—We begin by discussing the mean-field Hamiltonian derived from the $Sp(N)$ generalization of H . For the $N = 1$ case we can write the spin interaction in terms of Schwinger boson operators as $\vec{S}_i \cdot \vec{S}_j = b_{i\sigma}^\dagger b_{i\sigma'} b_{j\sigma'}^\dagger b_{j\sigma}$, where a sum over repeated indices σ and σ' (that take values \uparrow, \downarrow) is implied. The Hilbert space of the spin model is obtained by constraining the number of bosons on each site $b_{i\sigma}^\dagger b_{i\sigma} = 2S$. We can rewrite the interaction in terms of valence bonds created by the operator $\epsilon_{\sigma\sigma'} b_{i\sigma}^\dagger b_{j\sigma'}^\dagger$, where $\epsilon_{\uparrow\downarrow} = -\epsilon_{\downarrow\uparrow} = 1$. An arbitrary singlet state can be written in terms of some arrangement of these bonds with at most $2S$ bonds emanating from any lattice site. Generalizing these bond operators to N -flavors allows us to put a large number of bonds on a link. Since the Hamiltonian acting on a state changes at most two bonds per link, the relative change in the number of bonds goes like $1/NS$. In the large- N limit, their fluctuations are quenched. Therefore, we factorize the interaction in terms of valence bonds $Q_{ij} = \langle \epsilon_{\sigma\sigma'} b_{i\sigma,m} b_{j\sigma',m} \rangle / N$, where the *flavor* index $m = 1, 2, \dots, N$. We treat Q_{ij} as classi-

cal quantities, to obtain the mean-field Hamiltonian

$$H_{\text{MF}} = \frac{1}{2} \sum_{\langle ij \rangle} \left[N |Q_{ij}|^2 + \left(\epsilon_{\sigma\sigma'} b_{i\sigma,m}^\dagger b_{j\sigma',m}^\dagger Q_{ij} + H.c. \right) \right] + \sum_i \lambda_i \left(b_{i\sigma,m}^\dagger b_{i\sigma,m} - N\kappa \right) \quad (1)$$

Here Lagrange multipliers λ_i have been introduced to enforce the constraint on boson number $N\kappa$ at every site i , defining the *generalized spin length* $\kappa = 2S$. In what follows, we shall take λ_i to be spatially uniform $\lambda_i = \lambda$. We are interested in large enough values of κ to condense a flavor mode of the itinerant bosons, $\langle b_{i\sigma,m} \rangle = \sqrt{N} \delta_{1,m} x_{i\sigma}$, for long-range order to develop. The mean-field ground state energy (per flavor) is obtained by diagonalizing (1) by a canonical Bogoliubov transformation:

$$\frac{E_{\text{MF}}}{N} = \frac{1}{2} \sum_{\langle ij \rangle} \left[|Q_{ij}|^2 + (\epsilon_{\sigma\sigma'} x_{i\sigma} x_{j\sigma'} Q_{ij}^* + c.c.) \right] + \sum_i \lambda \left(|x_{i\sigma}|^2 - \kappa \right) \quad (2a)$$

$$+ \frac{1}{2} [\text{Tr} \sqrt{\lambda^2 \mathbb{1} - \mathbf{Q}^\dagger \mathbf{Q}} - N_s \lambda] \quad (2b)$$

Here N_s is the number of lattice sites, and (2b) is the zero-point energy contribution of the bosons. The exact mean-field ground state is obtained by a constrained minimization of the above expression. It can be systematically approached as an expansion in powers of $1/\kappa$. The leading contribution to the energy (of order κ^2) comes from terms in (2a), whose minimization simply relates the valence bonds to the condensate configuration in the classical ground state(s) of the Heisenberg Hamiltonian H with spin size $\kappa/2$. We will denote this configuration of bond variables with a superscript c : $\{Q_{ij}^c\}$. The quantum correction (of order κ) is provided by terms in (2b) for these bond configurations.

The ground states of the classical Hamiltonian (2a) consist of all spin configurations in which the spin vectors sum to zero in every tetrahedron. On general grounds we expect quantum corrections to select *collinear* ground states from the classical manifold [3, 4, 11]. We therefore restrict our attention to such states, in which each spin can be denoted by an Ising variable $\eta_i \in \{\pm 1\}$. Collinearity implies that, up to an arbitrary gauge transformation, $Q_{ij}^c = \kappa(\eta_i - \eta_j)/2$ and thus the bond variables are $\pm\kappa$ for every satisfied, antiferromagnetic (AFM) bond, and zero otherwise. Also, $\lambda^c = 4\kappa$ for all pyrochlore lattice classical ground states.

Loop expansion and effective Hamiltonian.—Next, we recast the first quantum correction to the mean field energy, Eq. (2b), for a given collinear classical ground state, into an effective Hamiltonian form where only some of the degrees of freedom remain [3]. Eq. (2b) can formally be Taylor-expanded

$$\frac{E_q}{N} = -\frac{1}{2} \sum_{m=1}^{\infty} \frac{(2m+1)!!}{2^m \lambda^{2m-1} m!} \text{Tr} (\mathbf{Q}^\dagger \mathbf{Q})^m \quad (3)$$

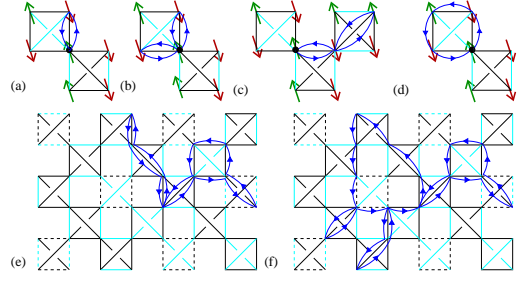


FIG. 1: (a)-(d) Schematic diagram of terms contributing to the constant term in the effective energy, due to $\text{Tr} \mathbf{Q}^2$ (a), and $\text{Tr} \mathbf{Q}^4$ (b,c,d). These are (001) projections, where the crossed squares are projected tetrahedra, and AFM bonds are shown in dark. All paths that do not contain loops, e.g. (a,b,c), can be viewed as paths on a coordination 4 Bethe lattice. (e)-(f): Examples of the two types of paths that we need to count, in order to calculate the effective Hamiltonian coefficients, as shown on a (001) slice of the pyrochlore lattice. The dashed lines represent bonds that connect to adjacent slices. (e) A decorated Bethe lattice path of length 14 contributing to $F(14)$ and (f) A path of length 22 containing a loop of length 8, contributing to $G(8, 14)$.

Since $|Q_{ij}/\kappa| = 1$ for AFM bonds, and zero otherwise, $\text{Tr}(\mathbf{Q}^\dagger \mathbf{Q}/\kappa^2)^m$ is equal to the number of closed paths of length $2m$, composed of AFM bonds. All terms in Eq. (3) depend solely on the structure of the network formed by AFM bonds. Note that since this network is bipartite, each nonzero element of $\mathbf{Q}^\dagger \mathbf{Q}$ is κ^2 .

In any collinear classical ground state, each tetrahedron has two up spins and two down spins, and four AFM bonds forming a closed loop (see Figs. 1a-d). This means that the local connectivity of the AFM network is identical for all states, and many closed paths only contribute state-independent terms to Eq. (3). For example, $\text{Tr} \mathbf{Q}^\dagger \mathbf{Q} = 4N_s \kappa^2$, for any classical ground state since the only paths of length 2 involve going to and fro on the same bond, and each site has four neighbors which have the opposite spin (see Fig. 1a). Similarly $\text{Tr}(\mathbf{Q}^\dagger \mathbf{Q})^2 = (16 + 12 + 4)N_s \kappa^4$, where the three terms correspond to the paths shown in Figs. 1b, 1c, 1d, respectively. All paths that do not involve loops, (e.g. those in Figs. 1a, 1b, 1c) can be viewed as paths on a Bethe lattice of coordination 4, and would contribute a constant term to the energy for all collinear classical ground states. The same is true for paths involving only trivial loops, in addition to the Bethe lattice path, as in Fig. 1d. Here, a “trivial” loop is the loop of length 4 that exists within any tetrahedron. The lowest order terms in expansion (3) that contribute a state-dependant term in the effective Hamiltonian are for $2m = 6$, since the shortest non-trivial loops are hexagons.

This leads us to parameterize the effective Hamiltonian in terms of the various non-trivial AFM loops.

$$\frac{E_q^{\text{eff}}}{N(\kappa/2)} = K_0 + K_6 \mathcal{P}_6 + K_8 \mathcal{P}_8 + K_{10} \mathcal{P}_{10} + \dots, \quad (4)$$

where $\{K_{2l}\}$ are numerical coefficients, and \mathcal{P}_{2l} is the number of non-trivial AFM loops of length $2l$, per site.

coefficient	analytical	numerically fitted
K_0	-0.59684	-0.59687
K_6	-3.482×10^{-3}	-3.522×10^{-3}
K_8	-3.44×10^{-4}	-3.76×10^{-4}
K_{10}	-3.59×10^{-5}	-4.5×10^{-5}
K_{12}	-3.8×10^{-6}	-5.5×10^{-6}

TABLE I: Coefficient values for Eq. (4), obtained analytically, and by an independent numerical fit to the energies in Fig. 2.

To evaluate the coefficients $\{K_{2l}\}$, we need to calculate two types of terms: (i) The number $F(2m)$ of closed paths of total length $2m$ on a decorated (with trivial 4-loops) coordination-4 Bethe lattice (Fig. 1e). (ii) The number $G(2l, 2m)$ of closed paths of length $2(m+l)$, involving a particular loop of length $2l$ with decorated Bethe lattice paths emanating from each site along the loop (Fig. 1f). Calculating these terms is a matter of tedious but tractable combinatorics. We find that the functions $F(2m)$, $G(2l, 2m)$ decay rapidly with m , allowing us to sum them in order to evaluate the coefficients to any accuracy in Eq. (4), using

$$K_0 = \sum_{m=0}^{\infty} F(2m), \quad K_{2l} = \sum_{m=0}^{\infty} G(2l, 2m). \quad (5)$$

We show the first five coefficients in Tab. I. Thus we have obtained an effective Hamiltonian that is parameterized solely by the number of AFM loops of various sizes. Note that the coefficients decay rapidly $K_{2l+2}/K_{2l} \approx 1/10$, which leads us to expect short loops to be the dominant terms in the expansion. This allows us, in principle, to calculate the energy, to any accuracy, for any member of an *infinite* ensemble of classical ground states. This represents a significant improvement over previous calculations that were always limited to small system sizes [9, 10].

Although we derived the effective Hamiltonian for collinear states, it turns out that, in fact, the classical tetrahedron zero sum rule implies that Eq. (4), with the coefficients in Tab. I, is valid for *any non-collinear* classical ground state, as well, with the generalized loop variables expressed as sums over non-trivial loops

$$\mathcal{P}_{2l} = \frac{1}{\kappa^{2l}} \sum_{(i_1 \dots i_{2l})} \text{Re}(Q_{i_1 i_2}^\dagger Q_{i_2 i_3} \cdots Q_{i_{2l-1} i_{2l}}^\dagger Q_{i_{2l} i_1}). \quad (6)$$

Unlike the collinear case, where the elements of $\mathbf{Q}^\dagger \mathbf{Q}$ could only take the values 0 or κ^2 , and thus each loop would contribute 0 or 1 to the sum (6), in the general case, the matrix elements of $\mathbf{Q}^\dagger \mathbf{Q}$ are complex.

Numerical results.—To verify the validity of the effective Hamiltonian (4), we calculated the energy for a large number of collinear classical ground states, as well as linear spin-wave ground states, obtained by a random flipping algorithm described elsewhere [11]. We find that the energies are remarkably well described by E_q^{eff} , even when we cut the expansion (4) off at $2l = 8$, as shown in Fig. 2. We used the

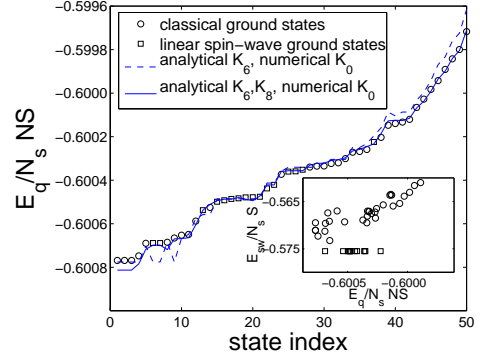


FIG. 2: Calculated energies E_q of 50 sample classical ground states (open symbols), 16 of which are harmonic spin-wave ground states (squares), along with E_q^{eff} , with $2l \leq 6$ (dashed line) and $2l \leq 8$ (solid line). The constant term K_0 was numerically fitted (see main text). The inset shows the linear spin-wave energy for the same states. Although the spin-wave energy tends to be lower for states with lower E_q , the large- N ground state need not be a spin-wave ground state.

coefficient values of Tab. I, but had to adjust the constant term K_0 separately for each choice of cutoff, in order to get a good fit [12]. In practice, this means that the effective Hamiltonian (4) is extremely useful for *comparing* energies of various states, even with a small cutoff, but requires many terms in order to accurately determine the energy. An independent 5-parameter numerical fit, to Eq. (4), up to $2l = 12$, gives the values shown in the right-hand column of Tab. I.

Now that we have an approximate formula for E_q , for any collinear classical ground state, we can systematically search these states, with large magnetic unit cells, to find a ground state. We conducted Monte Carlo simulations using a Metropolis loop flipping algorithm and the effective energy of Eq. (4), for various orthorhombic unit cells of sizes ranging from 128 to 3456 sites, with periodic boundary conditions. We find a minimum energy of $E_q/(N\kappa/2) = -0.60077N_s$ for a family of *nearly* degenerate states. They are composed of layers, that can each be in one of four arrangements, resulting in $\sim e^{cL}$ states, where L is the system size, and c is a constant. Each of these states has $\mathcal{P}_6 = N_s/3$, which is the maximum value that we find (but is *not* unique to these states), and $\mathcal{P}_8 = 23N_s/6$. Upon closer investigation, however, we find that a *unique ground state* (depicted in Fig. 3) is selected. The energy difference to nearby states is of order $10^{-7}N_s$, corresponding to the $2l = 16$ term.

Discussion.—It was noted by one of us [5] (see also [13]) that, in the pyrochlore, the degeneracy of ground states of the spin-wave quantum Hamiltonian, at the lowest order in $1/S$, is associated with a *gauge-like* symmetry. This symmetry characterizes the degenerate sub-manifold of collinear spin ground states by the condition

$$\prod_{i \in \square} \eta_i = -1, \quad (7)$$

for all non-trivial hexagons. Since the spin-wave theory is

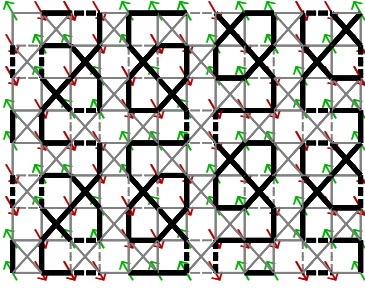


FIG. 3: The ground state of our large- N theory, as viewed in a (001) projection. Here, light (dark) bonds represent AFM (ferromagnetic) bonds (unlike in Fig. 1). The shown pattern is repeated along x and y directions, as well as in adjacent z slices. This state has a 48 site magnetic unit cell.

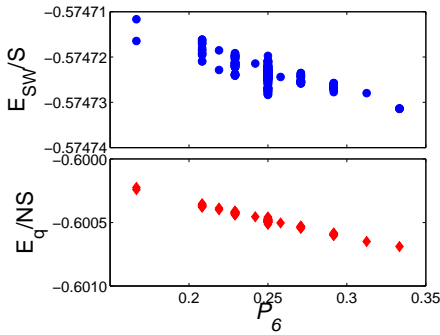


FIG. 4: Per-site large- N energies E_q calculated for various harmonic spin-wave ground states (bottom), compared to the per-site spin-wave energy obtained from an anharmonic calculation for $S = 1500$ (top). In both cases the lowest energy is for a state that maximizes the number of AFM hexagons.

expected to be exact in the limit of infinite S , the physical ground state must satisfy Eq. (7). The state depicted in Fig. 3, however, *does not*. Looking at the inset in Fig. 2, we find that states with negative hexagon products tend to have lower large- N energy than other states, since they tend to have more AFM loops, but this is not a strict rule. Thus it would seem that the $N \rightarrow \infty$, large- κ ground state cannot be the physical ($N = 1$) large- S ground state.

Nevertheless, if we restrict the large- N calculation to harmonic spin-wave ground states only, we find that the ordering of energies for various states is similar to preliminary anharmonic spin-wave results [6], and does predict the same ground state. As shown in Fig. 4, in both cases, the lowest energy among harmonic spin-wave ground state belongs to a state with the most AFM hexagons.

The effective Hamiltonian approach that we have outlined here can easily be applied to other lattices. In the checker-

board lattice, the energy is lowest for states that have the most AFM (square) non-trivial plaquettes. Thus, the non-degenerate ground state is clearly the (π, π) state in which *all* plaquettes are AFM [10]. In the kagomé case, all classical ground states are non-collinear. However, if we limit ourselves to coplanar arrangements, we find that Q_{ij} has the same absolute value for *all* of the lattice bonds, but the signs differ depending on the *chirality* of the triangle to which the bond (i, j) belongs. Therefore, the effective Hamiltonian (4), with the generalized variables (6), prefers classical ground states with negative product of triangle chiralities around all hexagons. One can thus conclude that the ground state is the $\sqrt{3} \times \sqrt{3}$ state, as large- N calculations have indeed found [9]. Let us also remark that our method can be generalized to long-range Heisenberg interactions which are relevant in the context of real materials like $\text{Tb}_2\text{Ti}_2\text{O}_7$ [1, 2].

Finally, it has been suggested that the disordered (*small- κ*) limit of the large- N approximation for the pyrochlore lattice also has a massive multiplicity of saddle-points [14]; an effective Hamiltonian similar to this paper's could organize the handling of this family.

UH and CLH acknowledge support from NSF grant DMR-0240953, and PS acknowledges support from the Packard foundation and the U.S. Dept. of Energy, under Contract No. W-31-109-ENG-38.

* Electronic address: uh22@cornell.edu

- [1] A. P. Ramirez, in *Handbook of Magnetic Materials*, edited by K. H. J. Buschow (Elsevier, Amsterdam, 2001), vol. 13, p. 423; Annu. Rev. Mater. Sci. **24**, 453 (1994).
- [2] H. T. Diep, ed., *Frustrated spin Systems* (World Scientific, Singapore, 2005).
- [3] C. L. Henley, Can. J. Phys. **79**, 1307 (2001).
- [4] E. F. Shender, Sov. Phys. JETP **56**, 178 (1982); C. L. Henley, Phys. Rev. Lett. **62**, 2056 (1989).
- [5] C. L. Henley (2005), cond-mat/0509005.
- [6] U. Hizi and C. L. Henley (2005), in preparation.
- [7] N. Read and S. Sachdev, Phys. Rev. Lett. **66**, 1773 (1991); S. Sachdev and N. Read, Int. J. Mod. Phys. B **5**, 219 (1991).
- [8] J.-S. Bernier, Y.-J. Kao, and Y. B. Kim, Phys. Rev. B **71**, 184406 (2005).
- [9] S. Sachdev, Phys. Rev. B **45**, 12377 (1992).
- [10] J.-S. Bernier, C.-H. Chung, Y. B. Kim, and S. Sachdev, Phys. Rev. B **69**, 214427 (2004).
- [11] U. Hizi and C. L. Henley (2005), cond-mat/0509008.
- [12] We could get a cutoff-independent constant term \tilde{K}_0 if we replaced \mathcal{P}_{2l} by $\tilde{\mathcal{P}}_{2l} = \mathcal{P}_{2l} - \langle \mathcal{P}_{2l} \rangle$, where $\langle \mathcal{P}_{2l} \rangle$ is the ensemble average of \mathcal{P}_{2l} , and took $\tilde{K}_0 = K_0 + \sum K_{2l} \langle \mathcal{P}_{2l} \rangle$.
- [13] O. Tchernyshyov, J. Phys. Condens. Matter. **16**, S709 (2004).
- [14] O. Tchernyshyov, R. Moessner, and S. L. Sondhi (2004), cond-mat/0408498.